Chemical Engineering Journal 145 (2008) 249–258

Contents lists available at ScienceDirect

Chemical Engineering Journal

journal homepage: www.elsevier.com/locate/cej

Axial voidage profiles and identification of flow regimes in the riser of a circulating fluidized bed

Mitali Das [a], Amrita Bandyopadhyay [b], B.C. Meikap [a,*], R.K. Saha [a]

[a] Department of Chemical Engineering, Indian Institute of Technology, Kharagpur 721 302, India
[b] Department of Chemical Engineering, Durgapur Institute of Advanced Technology and Management, Durgapur, India

ARTICLE INFO

Article history:
Received 26 February 2008
Received in revised form 9 April 2008
Accepted 16 April 2008

Keywords:
Circulating fluidized bed
Axial voidage
Fast fluidization
Choking velocity
Acceleration length

ABSTRACT

The hydrodynamics and flow regimes identification in fast-fluidized bed for single systems consisting of FCC, sand, coal, iron ore and mixed systems of FCC–sand and coal–iron ore were investigated in a perspex column (0.1016 m ID × 5.62 m high). The real voidage profiles have been found out by incorporating gas and solid friction factor and shear stress at the wall of column in the momentum balance equation. To study the flow regimes, the transport velocity (U_{tr}) was determined from the ($\Delta P_L/L$)–U_g–G_s relationship. The gas velocity at which solid hold-up in the upper dilute region exhibits a maximum value is defined as the fast transition velocity (U_{TF}) and the transition velocity to pneumatic transport as U_{FD}. In the present work, two correlations have been proposed for both the transition velocities. It has been found that the proposed correlation is in good agreement with experimental values of axial voidage.

1. Introduction

Fast-fluidized bed (FFB) has wide range of applications in petrochemical, mineral and metallurgical industries. A large number of reporting has been done on various aspects of CFB, especially on the hydrodynamics of the fast-fluidized bed [1–9]. Each CFB system is unique in its character and marked by some stable operational features. A CFB needs the creation of some special hydrodynamic conditions, namely a certain combination of superficial gas velocity, solid circulation rate, particle diameter, density of particle etc. which can give rise to a state wherein the solid particles are subjected to an upward velocity greater than the terminal or free fall velocity of the majority of the individual particles.

The fluidized bed displays different hydrodynamic flow regimes, from bubbling to pneumatic conveying depending on the superficial gas velocity. Various attempts have been made to see the flow regimes of gas solid suspensions on a single diagram in order to show how the regimes are related to each other. In practice, different workers had developed phase diagrams with widely differing view points of the same phenomena by plotting constant value lines of a parameter of interest as a function of two independent flow variables. Properties included gas flow rate, solids flux, voidage, pressure gradient, solid loading ratio etc. For specific piping system aeration rate, valve opening and overall system pressure drop are also important. However, studies in the fast fluidization regime are comparatively scant and hydrodynamic aspects like axial voidage profile are not well understood. Yerushalmi et al. [10] presented a qualitative fluidization map for fine solids in a sufficiently large bed where instability was absent. They plotted the slip velocity versus solids volumetric concentration, depicting different fluidization regimes, namely bubbling, slugging, turbulent and fast fluidization. The figure showed that a narrow turbulent regime exists, which was distinct from the fast bed regime. They also expand their phase diagram by including the dilute-phase pneumatic transport and choking. The phase diagram of Takeuchi et al. [11] defined the fast fluidization region as one bounded by two gas velocities that they termed U_{FF} and U_{DT}. The phase diagram was plotted for FCC particles with the co-ordinates of solid circulation rate and superficial gas velocity. U_{EF} was defined as the gas velocity below which solid circulation flux cannot be maintained constant while decreasing the riser gas velocity. They defined this as onset of fast fluidization regime. U_{DT} was characterized as the gas velocity at which pressure gradients measured at different heights in the riser; approach a constant value for given solids mass flux. Bi and Grace [12] proposed a practical definition of CFB regime: fast fluidization and dense phase conveying. Utilizing the variation of pressure gradient against the superficial gas velocity in both the dense and dilute phase of the bed, the transition velocities were found out. They proposed flow regime maps, which includes homogeneous dilute-phase flow, core-annular dilute-phase flow and fast fluidization. The choking velocity sets up the separation line between fast fluidization and

* Corresponding author. Tel.: +91 3222 283958; fax: +91 3222 282250.
E-mail addresses: bcmeikap@che.iitkgp.ernet.in (B.C. Meikap), rks@che.iitkgp.ernet.in (R.K. Saha).

1385-8947/$ – see front matter © 2008 Elsevier B.V. All rights reserved.
doi:10.1016/j.cej.2008.04.022

Nomenclature

Ar	Archimedes number, $d_P^2\rho_g(\rho_s-\rho_g)g/\mu^2$ (–)
$\bar{d}_P$	average particle diameter (m)
d_P	particle diameter (m)
D_t	column diameter (m)
f_g	gas friction factor
f_p	particle friction factor (–)
f_s	solids friction factor
FCC	spent FCC catalyst
g	acceleration due to gravity (m/s^2)
g_c	conversion factor
G_g	gas mass flow rate, $U_g\rho_g$ (kg/m^2 s)
G_s	solid circulation rate (kg/m^2 s)
G_{str}	solids flux at transport velocity (kg/m^2 s)
L	height of the column (m)
L_{acc}	accelerating (or mixing) length (m)
ΔP_L	pressure drop in lower part of column (kPa)
ΔP_T	total pressure drop in riser (kPa)
ΔP_u	pressure drop in upper part of column (kPa)
R	Reynolds number, $\rho_g d_p U_g/\mu$ (–)
R	Radius of the riser (m)
Re	Reynolds number, $d_p U_g \rho_g/\mu_g$
Re_p	particle Reynolds number, $d_p U_p \rho_g/\mu_g$
Re_t	Reynolds number at terminal settling velocity, $d_p U_t \rho_g/\mu_g$
t	time (s)
U_{ch}	choking velocity (m/s)
U_{DT}	transition velocity between turbulent and fast-fluidized bed (m/s)
U_{FD}	transition gas velocity between fast-fluidized bed and pneumatic transport (m/s)
U_{FF}	transition velocity between fast-fluidized bed and pneumatic transport (m/s)
U_g	superficial gas velocity (m/s)
U_s	solid velocity (m/s)
U_t	single particle terminal velocity (m/s)
U_t	terminal settling velocity (m/s)
U_{TF}	transition velocity between turbulent and fast fluidization (m/s)
U_{tr}	transport velocity (m/s)
W_s	solids rate (kg/s)

Greek letters

ε	voidage
μ	gas viscosity (kg/ms)
ρ_p	solid density (kg/m^3)
ρ_s	solid density (kg/m^3)
τ_w	wall shear stress (kPa/m)

dilute-phase pneumatic transport whereas the mechanism of transition from fast fluidization to dense-phase flow depends on the column and particle diameters. Llop et al. [13] has analyzed the correlations available for calculating different regime velocities. Based on their adequacy a simple map is proposed for the operating conditions over which each fluidization regime exists. Zijerveld et al. [14] have experimentally identified seven-fluidization regime of a pictorial fluidization diagram. Namkung and Kim [15] divided the fast fluidization regime into the fast transition and the fully developed fast fluidization region. They proposed a separating line between the two regions. Glass et al. [16] for the first time introduced particle image velocimetry (PIV) to produce vector maps of the gas-phase flow in the freeboard region of fluidized beds. Ge and Li [17] used energy minimization multi-scale model for physical mapping of fluidization regimes. Monazam and Shadle [18] analyzed the transient pressure drop data across the riser of CFB and found the three distinct operating regimes within the bed. Kim et al. [19] proposed a new regime map distinguishing the fast fluidization, dense suspension up flow (DSU) and dilute pneumatic transport flow regimes.

In the present study based on the analysis of generalized pressure gradient versus superficial gas velocity, both at the lower and upper sections of the bed, a practical definition of the flow regimes in a CFB, similar to that by Bai et al. [8] is presented. The fast transition velocity and the transition velocity to pneumatic transport have been correlated. The choking phenomenon has been studied from the pressure gradient versus superficial gas velocity as reported by Yousfi and Gau [20], Nakamura and Capes [21] and Das et al. [22].

The common features in each group of CFB application are that they are operated with bed solids that are not identical. However, no studies on wide range of particles in CFB have been reported so far. Therefore, in the present studies an attempt has been made to study the hydrodynamic characteristics of a CFB with mixed type of particles (binary systems) like FCC–sand and coal–iron ore and for single systems like sand of various sizes, FCC catalyst, iron ore and coal. Based on gas–solid momentum balance in the riser, a distinction between apparent and real voidage has been made. The effects of acceleration and friction on the real voidage have been estimated.

2. Experimental set-up and techniques

2.1. Experimental set-up and procedure

A circulating fluidized bed made of transparent perspex was used as the experimental apparatus. It consisted of a riser, a cyclone and a bag filter to separate the fines, a down comer, a slow bed and the transfer line connecting the slow and fast bed. The solids after passing through the fast bed in the riser gets separated in the cyclone and bag filter, descend downwards through the down comer and are collected in the slow bed and then transferred back into the riser. The CFB system being used here is schematically shown in Fig. 1(a) and pictorial set-up shown in Fig. 1(b). The detailed equipment characteristics are presented in Table 1. In actual practice air at controlled rates is supplied to the fast bed of CFB (0.1015 m diameter × 5.83 m in height) from a root blower through a multi-hole distributor plate having 12% open area. A small amount of air from the air bypass line is also sent to the slow bed to keep it at minimum fluidizing condition. For smooth transfer of suspended solids dispersed in air from riser column to slow bed and then send the solids back to the riser column a transfer line inclined at 60° with the horizontal is placed. The transfer line with a control valve is used to regulate the flow of solids independently. A butterfly valve is used to measure the solid circulation rate in the present case for obvious reasons like simplicity in operation and no loss in the solids that are circulated back into the riser. For the measurement of axial pressure around the CFB loop 21 pressure taps in the column wall are connected to water manometers. The superficial gas velocities into the riser and slow beds are measured by pressure drop measurements across standard calibrated orifice meters installed in the air supply lines. Under steady state conditions during experiment solid circulation rate, gas velocity in the riser and all the manometer readings for static pressure are noted. By varying the solid circulation rate and riser gas velocity, different sets of reading are taken.

Table 1
Equipment characteristics

Riser column	Slow bed column	Solid transfer line	Cyclone	Re-circulating column
Diameter = 0.1016 m Height = 5.62 m	Diameter = 0.2032 m Height = 1.88 m	Diameter = 0.1016 m Height = 0.42 m	Diameter = 0.258 m Height = 0.99 m	Diameter = 0.1016 m Height = 2.22 m

2.2. Materials and operating conditions

To study the hydrodynamic behaviour of single systems sand of various sizes (80, 300, 417, 522, 599 and 622 μm), FCC catalyst (120 μm), iron ore (166 and 140 μm) and coal (335 and 168 μm) have been used. The solid inventory to the bed has been made between 16 and 20 kg. For the mixed (binary) systems experiments were carried out with five different bed materials. The desired fractions of sample are prepared by grinding and screening the materials through the various wire mesh sieves. The first class of bed material is composed of quarts sand and spent FCC catalyst. Three samples of sand–spent FCC mixture each of 18.0 kg inventory with various mass percentage of sand ranging from 20% to 80% were used. Two class of bed material each of 18.0 kg comprises of a binary mixture of coal (80% by weight) and iron ore (20% by weight). The later class of bed material thus has differences both in sizes and densities and the same size but different densities. Superficial air velocity ranged between 2.01 and 4.681 m/s and corresponding mass fluxes were 12.5–50 kg/m^2 s. Experiments were carried out with five different bed materials along with the operating conditions that are listed in Tables 2 and 3 for single particle and mixed particle systems, respectively. The gas velocity in the riser can be varied by regulating the valves in the air lines. Solid circulation rate is controlled with the help of the

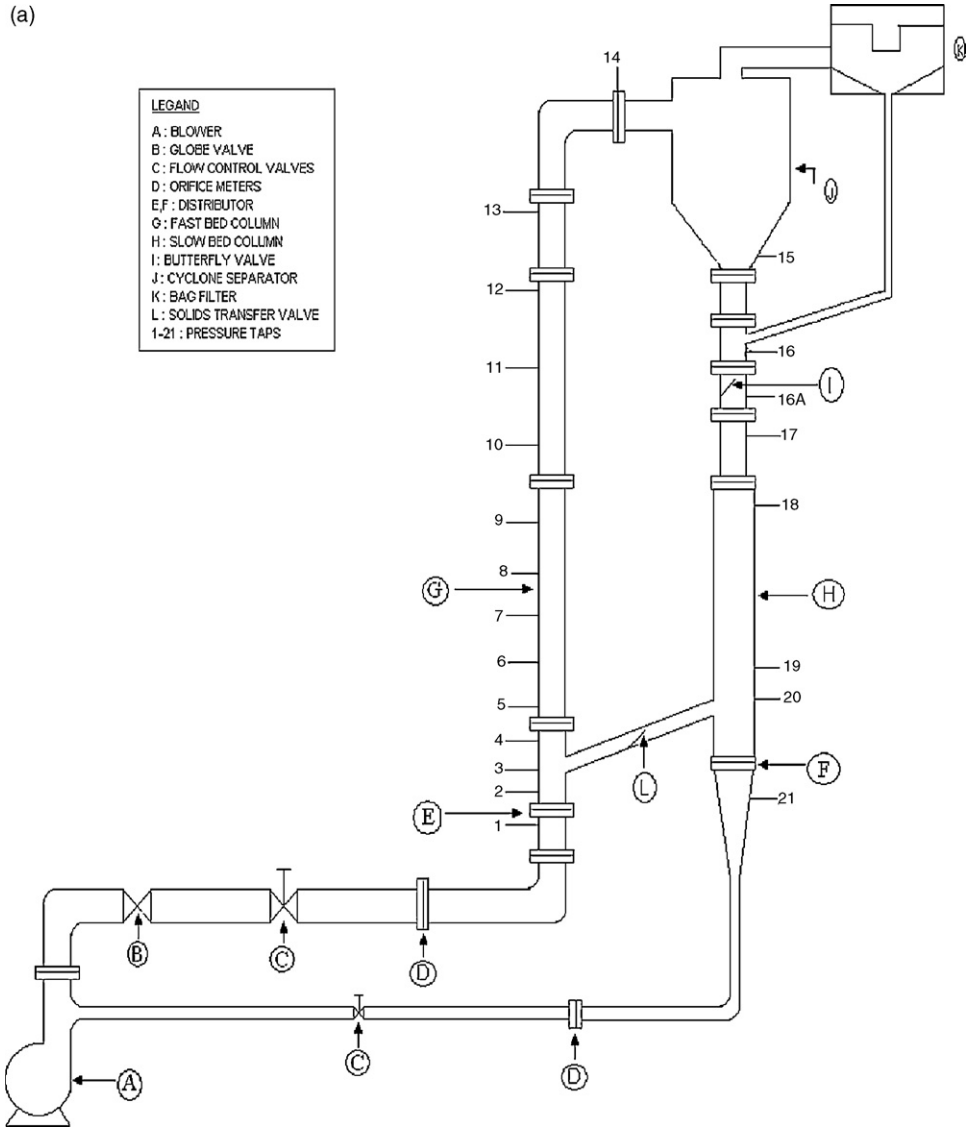

Fig. 1. (a) Schematic of the experimental set-up. (b) Pictorial view of experimental set-up.

Fig. 1. (*Continued*).

valve in the transfer line, which can be opened partially or fully. Solid circulation rate is measured with the help of butterfly valve. Solid circulation rate is measured by closing the valve momentarily and noting the solids accumulated on the valve plate against time.

3. Results and discussions

Experiments were conducted for static pressure profile and voidage profile in the velocity range 2.01–4.02 m/s and solid circulation rate 12.5–50.0 kg/m^2 s. Both group 'A' (FCC catalyst) and group 'B' (coal, iron ore and sand) materials and mixed systems consisting of FCC–sand and coal–iron ore have been used to study the voidage variation as a function of air velocity and solid circulation rate.

Figs. 2–5 show some of the voidage profiles along the riser height for the single systems. The voidages in these cases, termed as apparent voidages, have been calculated from the measured pressure gradient, assuming negligible acceleration effect and shear stress at the wall. Thus,

$$\frac{\Delta P}{z} = \rho_p(1-e)g \quad (1)$$

3.1. Effect of air velocity on voidage profile

The effect of air velocity on voidage profile is apparent in Fig. 2 at constant solid circulation rate. It shows that as velocity increases from 2.907 to 4.681 m/s, voidage increases from 0.97–0.99 to 0.98–0.999. This type of effect is observed because, as the air velocity increases, there will be a large carryover of particles and hence voidage increases.

3.2. Effect of solid circulation rate on voidage profile

The effect of solid circulation rate on voidage is apparent in Fig. 3 at constant velocity for the systems. As the solid circulation rate is increased from 24.75 to 50 kg/m^2 s, voidage profiles showed a decreasing trend along the riser height. This can be explained possibly, as the solid circulation rate increases, more amount of solid present along the riser height and hence voidage decreases.

3.3. Effect of particle size on voidage profile

Fig. 4 shows the effect of particle diameter on the voidage profile for air–sand system. At constant solid circulation rate and constant fast bed air velocity, voidage profile is being compared for particle diameters 300, 417, 521 and 622 μm. It is found that the bottom of the riser is denser for larger size particles. This can be explained as, at the riser bottom both the large and fine particles are present and fine particles are embedded in large diameter particles and hence the voidage decreases.

3.4. Effect of particle density on voidage profile

Fig. 5 shows the effect of particle density on the voidage profile for air–FCC, sand and iron ore. At a constant fast bed velocity of 2.01 m/s and solid circulation rate of 20.58 kg/m^2 s, the voidage

Table 2
Physical properties and operating conditions of bed materials (single particle system)

Bed materials	Particle size distribution	Particle diameter (μm)	CFB inventory (kg)	Density (kg/m^3)	Bed composition (%)	U_{mf} (m/s)	U_t (m/s)	ε_{mf}
Single particle system								
FCC	−30 + 52 = 7% −52 + 72 = 20.61% −72 + 120 = 72.39%	119.6	18	1672	100	0.05	0.40	0.38
Sand	−30 + 52 = 7.61% −52 + 72 = 23.46% −72 + 100 = 16.54% −100 + 200 = 52.39%	471.2	17	2668	100	0.131	4.01	0.44
Iron	−300 + 240 = 9.63% −240 + 200 = 12.36% −200 + 150 = 3.01% −150 + 120 = 13% −120 + 100 = 62%	166	20	5192	100	0.034	2.21	0.44
Coal	−30 + 52 = 65.87% −52 + 72 = 20% −72 + 100 = 14.13%	215	18	1150	100	0.078	2.08	0.45
Sand	−30 + 36 = 30.67% −36 + 52 = 29.33% −52 + 60 = 19.04% −60 + 72 = 6.31% −72 + 100 = 6.2%	300	17.5	2635	100	0.063	1.2	0.44
Sand	−30 + 52 = 7.61% −52 + 72 = 23.46% −72 + 100 = 16.54% −100 + 200 = 52.39%	417	18	2549	100	0.122	1.2	0.45
Sand	−22 + 25 = 100%	522	18	2549	100	0.122	2.86	0.45
Sand	−16 + 22 = 7.61% −22 + 30 = 20.13% −30 + 44 = 21.64% −44 + 60 = 29.22% −60 + 72 = 10.17% −72 + 100 = 3.9% −100 + 200 = 2.38%	622	19.5	2590	100	0.122	1.4	0.45

profile has been compared for three systems with iron ore being the densest of the three. It is found that with iron ore the riser bed is less dense as the riser height rises. This can be explained that dense particles are heavier enough to move along the riser and as a result voidage is more pronounced for them.

4. Real voidage profile in fast-fluidized bed

The riser can be divided into three sections: an acceleration zone, a developed flow zone and a deceleration zone. The deceleration zone is normally present when the riser is equipped with an abrupt exit configuration. In the present case, the riser was fitted with a smooth elbow-type of exit and so the deceleration zone is absent. The developed flow zone has been extended up to the exit end. Neglecting gas inertia and gravitation, the gas–solid mixture momentum equation can be written as

$$\frac{dP_T}{dL} + \frac{4\tau_w}{D_t} - \rho_p(1-\varepsilon)g + w_s\left(\frac{dU_S}{dL}\right) = 0 \quad (2)$$

Expressing the wall shear stress in terms of solid and gas component wall friction factors, f_s and f_g, Eq. (2) can be integrated between

Table 3
Physical properties and operating conditions of bed materials (mixed particle system)

Bed materials	Particle size distribution	Particle diameter (μm)	CFB inventory (kg)	Density (kg/m^3)	Bed composition (%)	U_{mf} (m/s)	U_t (m/s)	ε_{mf}
Mixed particle systems								
FCC–sand		FCC (119) Sand (471)	16	1805	80%-FCC 20% sand	0.131	2.16	0.44
FCC–sand		FCC (119) Sand (471)	18	2049	50%-FCC 50% sand	0.131	2.16	0.44
FCC–sand		FCC (119) Sand (471)	18	2365	20%-FCC 80% sand	0.131	2.16	0.44
Coal–iron ore		Coal (335) Iron ore (140)	20	1780.87	80%-coal 20%-iron ore	0.122	1.4	0.45
Coal–iron ore		Coal (168) Iron ore (166)	20	1780.87	80%-coal 20%-iron ore	0.122	1.4	0.45

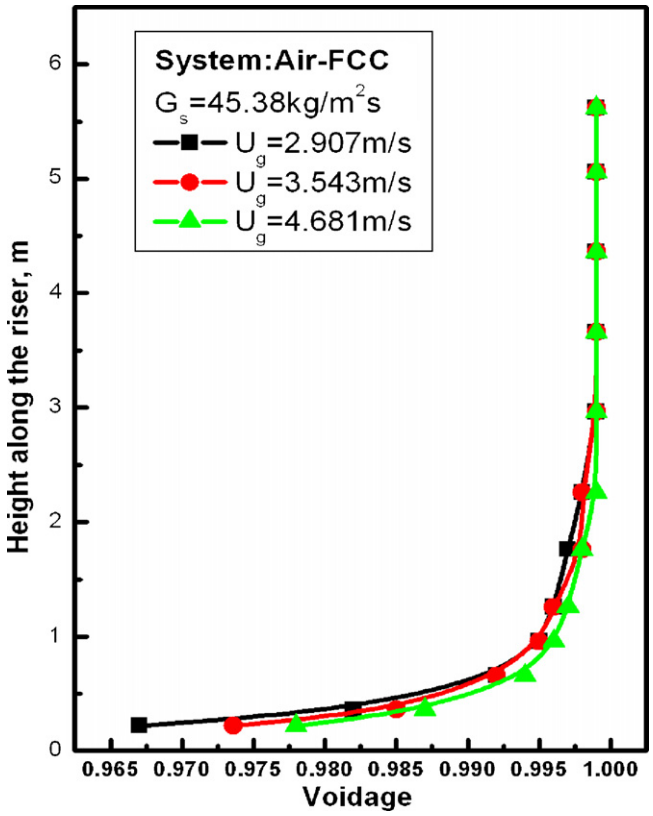

Fig. 2. Voidage profile along the riser: effect of superficial gas velocity (system: air–FCC).

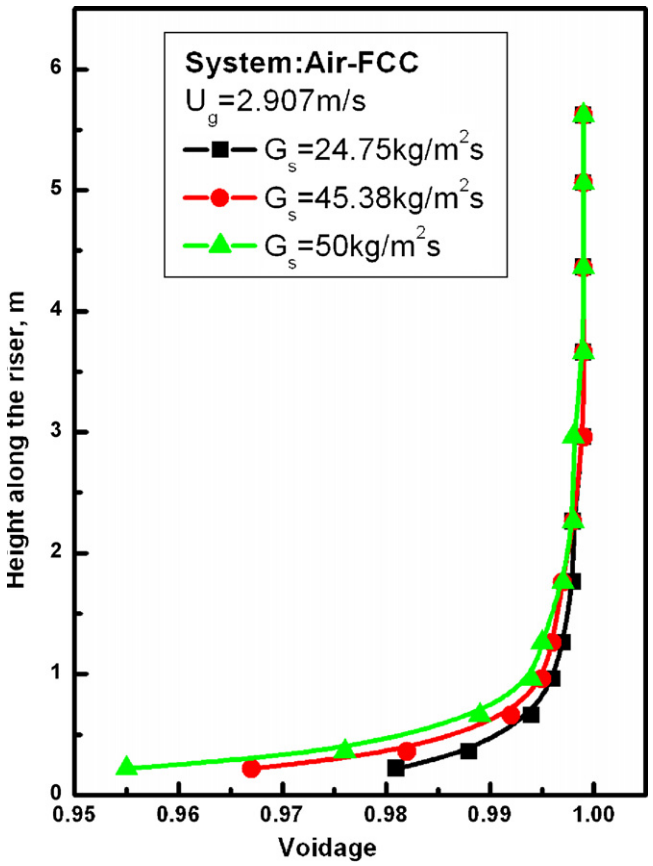

Fig. 3. Voidage profile along the riser: effect of solid circulation rate (system: air–sand).

two points of the riser and written in final form:

$$\Delta P_T = \int_0^L \rho_p(1-\varepsilon)g\,dL + \left[\frac{G_s^2}{\rho_p(1-\varepsilon)}\right]_0^L + \int_0^L \frac{2f_s G_s^2}{\rho_p(1-\varepsilon)D_t}\,dL + \int_0^L \frac{2f_g G_g^2}{\rho_g \varepsilon D_t}\,dL \quad (3)$$

4.1. Voidage in the accelerating zone

At the riser bottom, in the present case, an acceleration zone persists up to a considerable portion of the riser length. Up to the length of acceleration zone, (L_{acc}), the total pressure drop can be written on simplification of Eq. (3) as:

$$\Delta P_T = \int_0^{L_{acc}} \rho_p(1-\varepsilon)g\,dL + \int_0^{L_{acc}} \frac{2f_s(1-\varepsilon)\rho_p U_s^2}{D_t}\,dL + \int_0^{L_{acc}} \frac{2f_g \varepsilon \rho_p U_g^2}{D_t}\,dL + \rho_p(1-\varepsilon)U_S^2 \quad (4)$$

The acceleration pressure drop thus consists of four terms: solid particle gravity, gas friction, solid friction and kinetic energy of solid particles at the accelerating length. The voidage (real) ε, in the above equation can be evaluated if the particle velocity U_s is known. The solid particle velocity in the present case is obtained from the relationship:

$$U_s = \frac{G_s}{\rho_p(1-\varepsilon)} \quad (5)$$

Further, to solve for the evaluation of real voidage in the acceleration zone of the riser using Eq. (4), the solid friction factor f_s and the gas friction factor f_g are required. Yang [23] proposed the following empirical equation for the vertical pneumatic conveying:

$$f_s\frac{\varepsilon^3}{(1-\varepsilon)} = 0.0126\left[(1-\varepsilon)\frac{Re_t}{Re_p}\right]^{-0.979}, \quad \frac{U_t}{U_s} > 1.5 \quad (6)$$

$$f_s\frac{\varepsilon^3}{(1-\varepsilon)} = 0.0410\left[(1-\varepsilon)\frac{Re_t}{Re_p}\right]^{-1.021}, \quad \frac{U_t}{U_s} < 1.5 \quad (7)$$

Eqs. (4)–(7) were solved iteratively to evaluate ε (real).

4.2. Voidage in fully developed zone

Above the accelerating zone, the kinetic energy of solid particles can be neglected. Incorporating the static head for gas, Eq. (4) is modified to

$$\Delta P_T = \int_{L_{acc}}^{L} \rho_p(1-\varepsilon)g\,dL + \int_{L_{acc}}^{L} \rho_g \varepsilon g\,dL + \int_{L_{acc}}^{L} \frac{2f_s(1-\varepsilon)\rho_p U_s^2}{D_t}dL + \int_{L_{acc}}^{L} \frac{2f_g \varepsilon \rho_g U_g^2}{D_t}\,dL \quad (8)$$

The fully developed zone in the riser section (indicated by apparent voidage profile) of a circulating loop appears to behave like a dilute-phase vertical pneumatic transport line and so, the correlation developed by Yang [23] for such beds can be employed. Thus, the particle velocity, beyond the acceleration region, can be

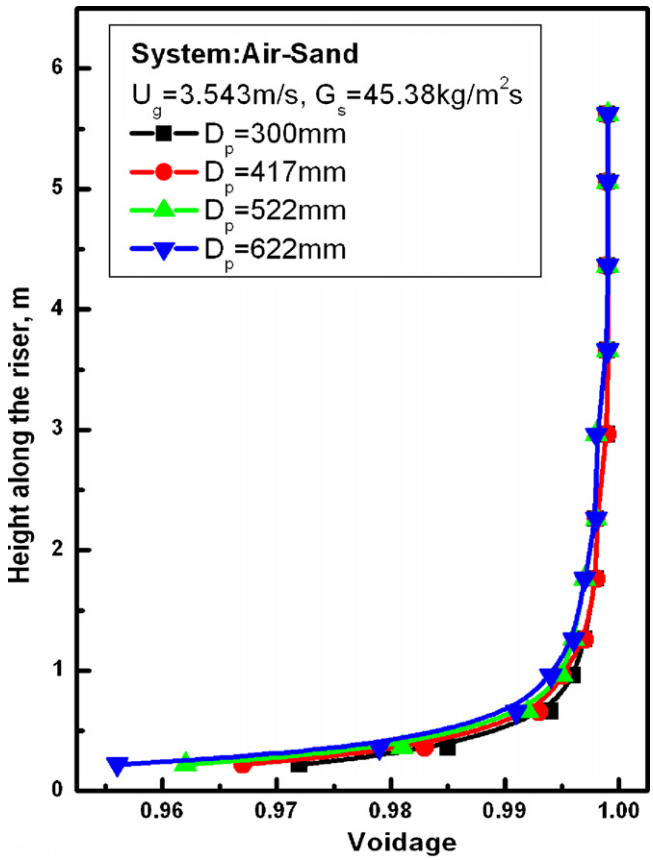

Fig. 4. Voidage profile along the riser: effect of particle diameter (system: air–sand).

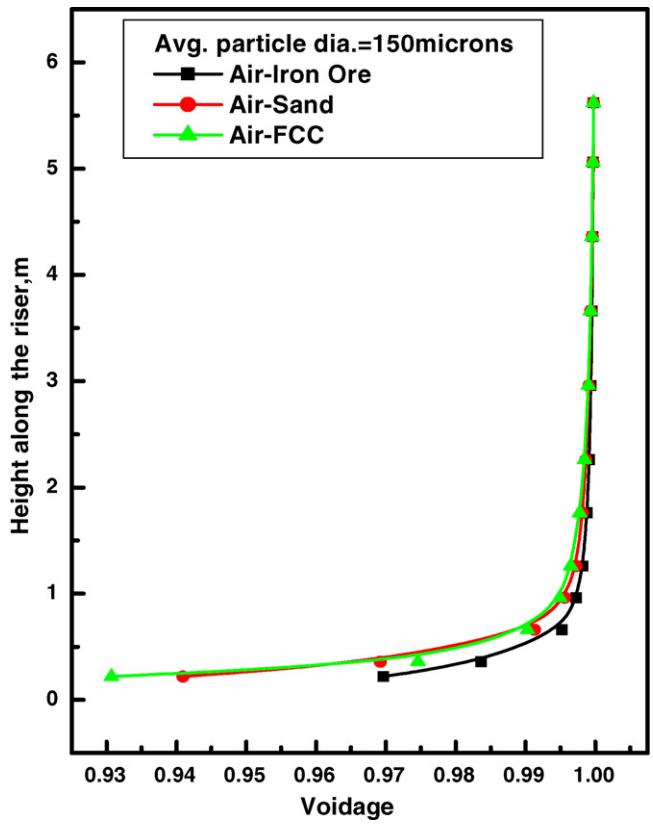

Fig. 5. Voidage profile along the riser: effect of particle density.

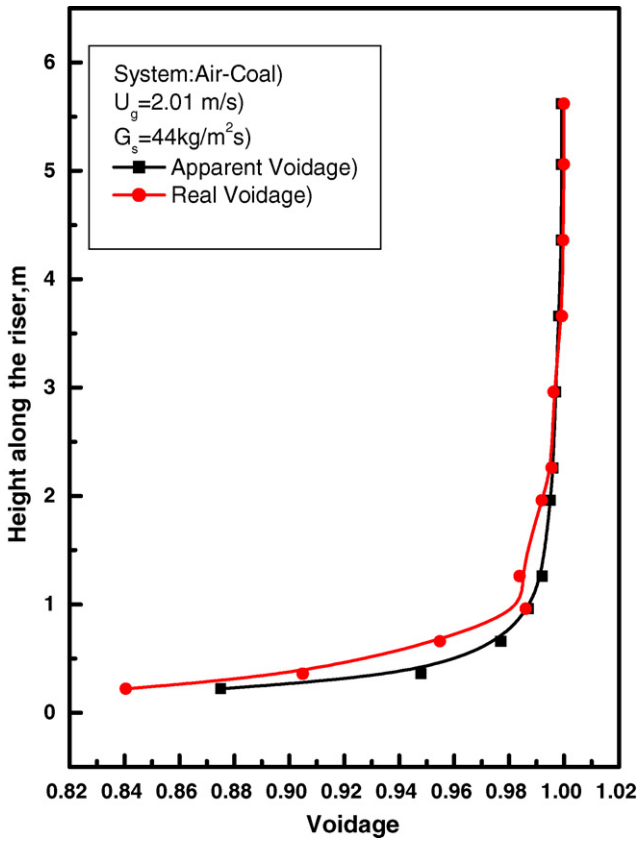

Fig. 6. Comparison of apparent and real voidages.

expressed as

$$U_S = U_g - U_t\sqrt{\left(1+\frac{f_s U_s^2}{2gD_t}\right)}\varepsilon^{4.7} \quad (9)$$

Eq. (8) in conjunction with Eqs. (9), (6) and (7), are solved iteratively for the evaluation of voidage (real) in the developed zone. It is evident that there is perceptible difference between the apparent and real voidages. This is more evident when the data are plotted as presented in Fig. 6. It can be seen from above figure that above 1.9–2.26 m riser height, the apparent and real voidage profiles merge together.

5. Identification and characterization of various regimes in a CFB

To identify various regimes in a CFB qualitatively, Bai et al. [8] used the generalized pressure gradient versus superficial gas velocity diagram showing plots of both the lower and upper sections of the bed. This is shown in the Fig. 7. When the gas velocity is low, the bed operates either in the bubbling or turbulent fluidization regime. In this case, a distinct bed surface separates the bed from the free board where the concentration of solid is very low. As the gas velocity is increased above the turbulent fluidization regime, the solids from dense bottom are elutriated thereby sharply decreasing the pressure drop per unit length ($\Delta P_L/\Delta x$). This is represented by OA in the figure. Consequent upon this decrease, the solids in the upper free board accumulate more and more so that the pressure drop per unit length ($\Delta P_U/\Delta x$) increases significantly (shown by CT in the Fig. 7(a)). Finally, a gas velocity is approached when it becomes saturated with solids. At this instant, there will be rapid dilution due to sharp increase in the rate of solid entrainment and the recycle

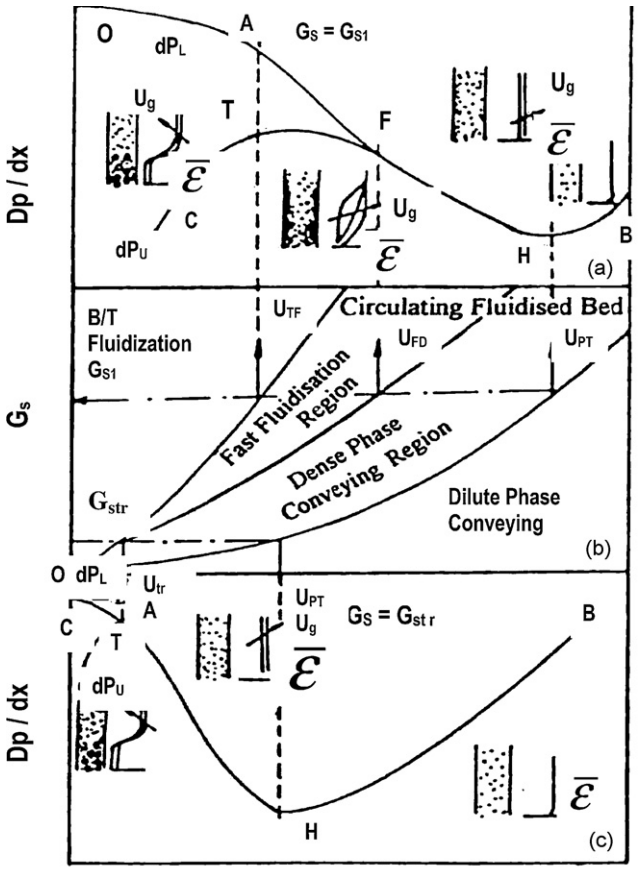

Fig. 7. Generalized pressure gradient versus superficial gas velocity for lower and upper bed-sections.

cease due to absence of solids. If the gas velocity is increased further, both ΔP_L and ΔP_U curves move downwards and merge at point F (Fig. 7(a)). After certain velocity, the difference between the dense phase at the bottom and dilute phase at the top will no longer exists and a transition to dense phase conveying will occur.

The central point in Fig. 7(a) (ATF) represents the fast fluidization zone. It strongly depends on the solid circulation rate for the given gas–solid flow system. The difference between the transition velocities (U_{TF} and U_{FD}) decreases with a decrease in solid circulation rate (Fig. 7(b)). If the solid circulation rate is very low ($G_s < G_{str}$), the transition from bubbling/turbulent bed to fast fluidization may not occur at all and the bed transforms directly into dense phase conveying system (Fig. 7(c)). This condition (U_{tr} and G_{str}) is referred to as the minimum condition for fast fluidization.

It is obvious that a fast-fluidized bed operates between U_{TF} and U_{FD}. But if G_s is reduced, the difference between U_{TF} and U_{FD} also narrows down and there may be a value of G_s when U_{TF} and U_{FD} become equal and the bed transforms from fast bed to pneumatic conveying. Thus, to operate a CFB in the fast-fluidized regime, the following conditions should be met:

$$U_g > U_t,\ G_s > G_{str} \quad \text{and} \quad U_{TF} < U_g < U_{FD} \tag{10}$$

Plots of pressure and voidage profiles along the length of riser have been discussed. Based on these data, pressure drop per unit length of the riser can be obtained. The plots of $(\Delta P_L/L)$–U_g–G_s remain, in the present case, in the ATF region (Fig. 7), i.e. fast-fluidized zone and dense phase conveying zone. Some of the plots (Figs. 8–10) of $(\Delta P_L/L)$–U_g–G_s have been given for single and mixed systems which also clearly support the statement.

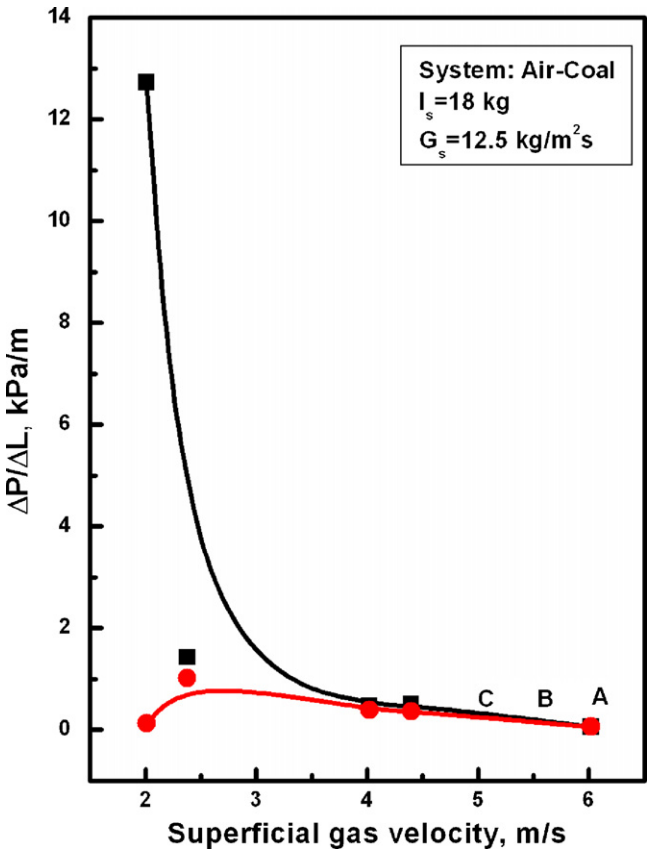

Fig. 8. Variation of $\Delta p/\Delta L$ with superficial gas velocity (system: air–coal).

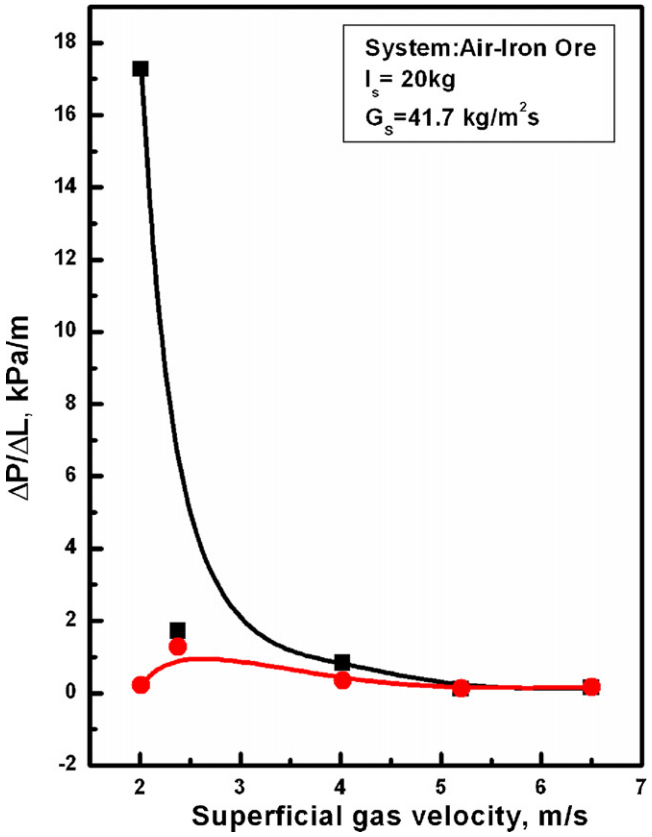

Fig. 9. Variation of $\Delta p/\Delta L$ with superficial gas velocity (system: air–iron ore).

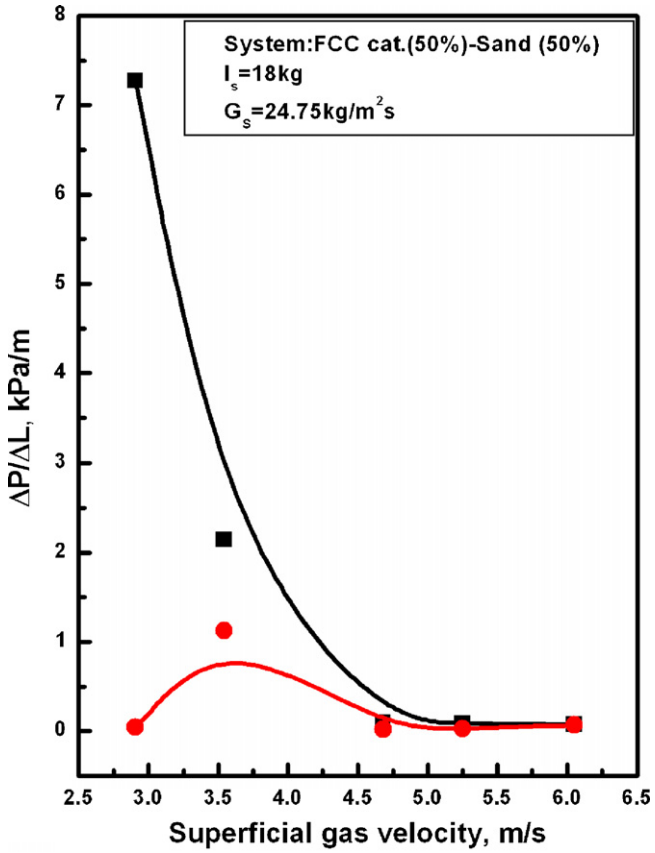

Fig. 10. Variation of $\Delta p/\Delta L$ with superficial gas velocity (system: FCC–sand).

5.1. Transition velocities

The experiments have shown that the transition velocity U_{TF} depends not only on the gas–solid properties but also on the solid circulation rate and bed diameter. Based on these data, the following empirical correlation for U_{TF} has been proposed (which has a standard error of estimation of 0.14 and correlation coefficient of 0.91).

$$Re_{TF} = 0.541(\mathrm{Ar})^{0.47}\left(\frac{G_s}{\rho_g U_t}\right)^{0.03} \quad (11)$$

where,

$$63 \le \mathrm{Ar} \le 927 \quad \text{and} \quad 2 \le \left(\frac{G_s}{\rho_g U_t}\right) \le 254$$

The transition velocity (U_{FD}) between fast fluidization and dense phase conveying is also affected by the solid circulation rate, bed material properties and column diameter. As in the previous case, the present data has been used to develop the following correlation (with a standard error of estimation of 0.14 and correlation coefficient of 0.915).

$$Re_{FD} = 0.572(\mathrm{Ar})^{0.48}\left(\frac{G_s}{\rho_g U_t}\right)^{0.0043} \quad (12)$$

where,

$$64 \le \mathrm{Ar} \le 10897 \quad \text{and} \quad 2 \le \left(\frac{G_s}{\rho_g U_t}\right) \le 97$$

5.2. Choking velocity (U_{ch})

Choking represents a demarcation between operationally and hydrodynamically different flow regimes. Choking thus, can be defined as the point in $\Delta P/L$ versus U_g plot, where either a slight decrease of transport velocity at the same solids rate or a slight increase of solids rate at a fixed transport velocity will increase the pressure drop in the transport line exponentially. Because of substantial pressure fluctuations in the riser at choking condition, determination of the choking point is quite difficult. Yousfi and Gau [20] defined choking as a state in which the solids slugs extended over the entire pipe cross-section that could visually be observed. Nakamura and Capes [21] observed slugging phenomena occurring in a vertical gas–solid flow much below the velocity, at which internal solids circulation occurs. To characterize the choking phenomena quantitatively, the local static pressure was measured in the upper (ΔP_u between pressure taps 10 and 11) and lower (ΔP_L, between taps 3 and 4) sections of the riser column.

In uniform dilute flow, the frictional pressure drop prevails and there is no drift between mean values of pressure measured in the upper and lower sections of the riser (Fig. 8). With decreasing gas velocity, formation of an annular dense flow can be observed, with the layer of particles in the vicinity of the wall flowing downwards. An increase of particle concentration in this layer leads to the formation of cluster particle, which can transfer to the lean core at the center of the riser. Further decrease in gas velocity leads to the segregation boundary in the column. A local hold-up increases throughout in the riser axially as well as radially. At this point, considerable difference can be observed between ΔP_L and ΔP_u (Figs. 9–10). If the gas velocity is reduced below C, particles start to accumulate at the bottom section of the column due to imbalance between the solids feed rate and the transport capacity of the gas. This may be defined as the choking effect. The velocity U_{ch} is

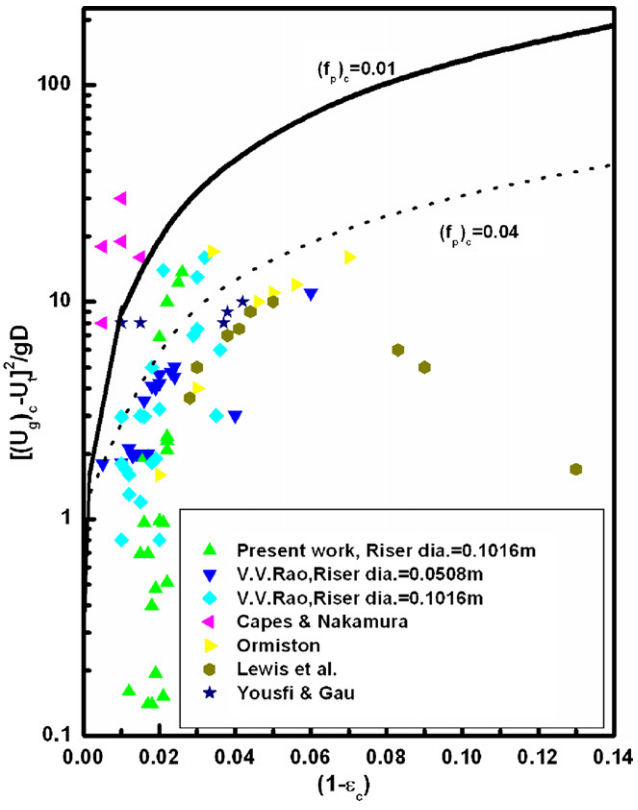

Fig. 11. Comparison of calculated and experimental choking velocity (U_{ch}).

called the choking velocity. Below this velocity, the solids form a bubbling (or slugging) dense bed. The local pressure drop at the bottom (ΔP_L) increases steeply (due to higher solid hold-up) with decreasing U_g. However, the local pressure drops (ΔP_u), measured above the bubbling dense bed line, decreases with decreasing U_g due to low transport capacity of the gas. Thus, the $(\Delta P/L)_u$ versus U_g plots can be used to determine the value of U_{ch}.

All the choking data available in literature have been plotted in Fig. 11 for the sake of comparison. It is found that these data fall between the two demarcating lines, namely the particle friction factor at choking $(f_p)_c$ equal to 0.01 and 0.04. The majority of the data fit with the line at $(f_p)_c = 0.04$. The onset of internal solids circulation fit better with the line at $(f_p)_c = 0.01$. Barring a few exceptions, most of the present data lie well within these two demarcating boundaries.

6. Conclusions

In the present investigation, the hydrodynamics of fast fluidization have been studied thoroughly by using Geldart's group A, group B and group A and B mixed type of particles in a CFB system. The hydrodynamics have been studied with wide size distributions of particles. The longitudinal voidage profiles indicate an exponential decay along the riser of CFB. Based on the momentum analysis of gas–solid mixture along the riser, an attempt has been made to predict the 'real' voidages both at the bottom and top of the riser. The difference noted between the apparent and real voidages at the bottom of the bed has been attributed to the accelerating particle pressure drop. Results indicate that above 1.9–2.26 m riser height, the apparent and real voidage profiles merge together.

Wide size distributions of particles are likely to affect the regime transition. Regime identification as well as chocking phenomena presented for large size range particles. Correlations for regime transition velocities (onset of fluidization and beginning of dense phase transport velocity) have been proposed.

References

[1] H. Arastoopour, D. Gidaspow, Analysis of IGT pneumatic conveying data and fast fluidization using a thermohydrodynamic model, Powder Technol. 22 (1) (1979) 77–87.
[2] M. Das, B.C. Meikap, R.K. Saha, Dry beneficiation of iron ore and coal in a fast fluidized bed—a case study, Int. J. Chem. Sci. 5 (4) (2007) 1691–1700.
[3] E.U. Hartge, K. Luecke, J. Werther, The role of mixing in the performance of CFB reactor, Chem. Eng. Sci 54 (22) (1999) 5393–5407.
[4] L. Hongzhong, H. Rouyu, W. Zhaolin, Fluidizing ultrafine powders with CFB, Chem. Eng. Sci. 54 (1999) 5609–5615.
[5] H.T. Bi, P.C. Su, Local phase holdups in gas–solid fluidization and transport, AIChE J. 9 (2001) 2025–2031.
[6] H. Li, H. Tong, Multi-scale fluidization of ultrafine powders in a fast-bed-riser/conical-dipleg CFB loop, Chem. Eng. Sci. 59 (8–9) (2004) 1897–1904.
[7] E. Santhosha, T. Narsaiah, V.V. Rao, Modelling of flow structure near the wall in circulating fluidized bed, Ind. Chem. Eng. 49 (1) (2007) 38–44.
[8] D. Bai, y. Jin, Z. Yu, Flow regimes in CFB, Chem. Eng. Technol. 16 (1993) 307–313.
[9] M. Das, M. Banerjee, R.K. Saha, Segregation and mixing effects in the riser of a circulating fluidised bed, Powder Technol. 178 (2007) 179–186.
[10] J. Yerushalmi, N.T. Cankurt, D. Geldart, Flow regimes in vertical gas–solid contact systems, AIChE Symp. Ser. 176 (1978) 1–13.
[11] H. Takeuchi, T. Hirama, T. Chiba, J. Biswas, L.S. Leung, A quantitative definition and flow regime diagram for fast fluidization, Powder Technol. 47 (1986) 195–199.
[12] H.T. Bi, J.R. Grace, Flow Regime diagrams for gas–solid fluidization and upward transport, Int. J. Multiphase Flow 21 (6) (1995) 1229–1236.
[13] M.F. Llop, J. Arnaldos, J. Casal, Fluidization at vacuum conditions: a generalized equation for the prediction of minimum fluid velocity, Chem. Eng. Sci. 51 (23) (1996) 5149–5157.
[14] R.C. Zijerveld, F. Johnsson, A. Marzocchella, V.D. Bleek, Fluidisation regimes and transitions from fixed bed to dilute transport flow, Powder Technol. 95 (1998) 185–204.
[15] W. Namkung, S. Kim, Flow regimes and axial pressure profiles in a CFB, Chem. Eng. J. 72 (1999) 245–252.
[16] D.H. Glass, S.J.L. Rix, M.I. Yorquez-Ramirez, PIV investigations of flow structures in the fluidized bed freeboard region, Powder Technol. 120 (2001) 2–11.
[17] W. Ge, J. Li, Physical mapping of fluidization regimes-the EMMS approach, Chem. Eng. Sci. 57 (18) (2002) 3993–4004.
[18] E.R. Monazam, L.J. Shadle, A transient method for characterizing flow regimes in a circulating fluidized bed, Powder Technol. 139 (2004) 89–97.
[19] S.W. Kim, G. Kirbas, H. Bi, C.J. Lim, J. Grace, Flow behaviour and regime transition in a high density CFB riser, Chem. Eng. Sci. 59 (2004) 3955–3963.
[20] Y. Yousfi, G. Gau, Aerodynamique de l'ecoulement vertical de suspensions concentrees gaz-solides—I. Regimes d'ecoulement et stabilite aerodynamique, Chem. Eng. Sci. 29 (1974) 1939–1956.
[21] K. Nakamura, C.E. Capes, Vertical pneumatic conveying: a theoretical study of uniform and annular particle flow models, Can. J. Chem. Eng. 51 (1973) 31–38.
[22] M. Das, B.C. Meikap, R.K. Saha, Characteristics of axial and radial segregation of single and mixed particle system based on terminal settling velocity in the riser of a circulating fluidized bed, Chem. Eng. J. 145 (2008) 32–43.
[23] W. Yang, A correlation for solid friction factor in vertical pneumatic conveying lines, AIChE J. 24 (1978) 548–552.